Linear stability implications of chevron geometry modifications for turbulent jets

Aniruddha Sinha[1][*], Abhinav Rajagopalan[1][†] and Shreeni Singla[2][‡]

[1]*Aerospace Engineering, Indian Institute of Technology Bombay, Powai, Mumbai 400076, INDIA*
[2]*Mechanical Engineering, PEC University of Technology, Chandigarh 160012, INDIA*

Chevrons or nozzle serrations are being deployed for reducing the mixing noise from jets. We study the effect of chevron geometry modifications on linear instability wavepackets within the turbulent jet plume. The wavepackets have been linked to the loudest low-frequency low-azimuthal mode number components of noise, especially in the aft angles. We use RANS to model the effect of the chevron variations on the turbulent mean flow field (that supports the instabilities). Subsequently, parabolized stability equations (PSE) is used to ascertain the effect of these base flow changes on the wavepackets. We find that increasing the chevron impingement weakens the wavepackets whereas increasing the chevron count strengthens them. These trends match the corresponding acoustic field effects observed in experiments. The proposed RANS-PSE model may thus be used to efficiently arrive at an optimum chevron nozzle design for noise reduction.

I.   Introduction

The turbulent mixing noise from jet engines is one of the most annoying loud noises encountered routinely by man. Of the many technologies developed to mitigate this noise, chevrons (serrations) at the lip of the nozzle pose one of the most feasible solutions that have actually been deployed on commercial aircraft. The design of chevrons (as well as other proposed noise mitigation technologies) for optimal noise reduction, is primarily through trial and error involving costly experimentation[1,2,3,4] and/or numerical simulation (typically large-eddy simulation, LES).[5,6,7] Another approach that is sometimes favored is empirical noise models that invoke an acoustic analogy and take as input an estimate of the scales of turbulence fluctuations in the jet plume, usually using Reynolds-averaged Navier Stokes (RANS) simulations.[8,9] Here, we propose to build the foundation for a third alternative that is explained now.

The aft-angle noise spectrum of jet engines is dominated by low frequencies and low azimuthal Fourier modes.[10] The latter components have been linked to the large-scale coherent structures convecting in the jet plume.[11] The primary stochastic features of these structures (average amplitude envelope and convection speed) have been successfully modeled as linear instability modes of the turbulent mean flow field, as recently reviewed in Ref. 11. Although this hypothesis had been proposed several decades ago,[12,13,14] the recent availability of detailed experimental data and realistic large-eddy simulation results have leant strong support to it and spurred further developments. Good agreement between the linear instability theory and empirical data was reported for round jets, both subsonic[15,16,17] and supersonic.[18] Encouraging validation was also reported in more complex jets like coaxial jets[19] and chevron jets,[20,21] the latter being of particular relevance to this article.

Spatial linear hydrodynamic stability analysis takes a base flow as input to predict the spatial evolution of perturbations (typically of a certain frequency) to the base flow. There are various levels of sophistication in the stability models. In parallel-flow spatial linear stability theory (LST), the base flow is assumed to be locally parallel in the primary convective (axial) direction, and eigen-solutions found at different axial stations may be composed together into a global portrait of the instability envelope.[15] At the other end

---

[*]Assistant Professor; AIAA Member; Corresponding author: as@aero.iitb.ac.in
[†]Graduate student
[‡]Undergraduate student

American Institute of Aeronautics and Astronautics

of the spectrum, global stability theory makes no assumptions on the base flow, and instead, solves for the instability envelope in the temporal stability setting.[22] In between these two extremes, parabolized stability equations (PSE),[23] as well as the method of multiple scales,[14,24] assume a mild non-parallelism of the base flow and solve a space-marching equation set to approximate the instability envelope. In this article we will use PSE to model the average spatial evolution of large scale coherent structures in jets issuing from chevron nozzles, as has been pursued in Ref. [21] and Ref. [25].

Our objective is to understand the influence of the chevron geometry on the spatial evolution of large-scale coherent structures in the jet. The first attempt in this endeavor was simultaneously reported in Ref. [26] and Ref. [27]. LST was used to analyze the modification of growth rate and phase speed of the Kelvin-Helmholtz (K-H) instability in a variety of mean flow profiles. The nominal condition was chosen as the Mach 0.9 cold jet issuing from the SMC001 nozzle tested at NASA SHJAR,[1] with the profile extracted at two-jet-diameters downstream of the nozzle exit. The mean flow has a serrated structure due to the impingement of the chevrons in to the shear layer. It was parameterized in terms of the serration depth, serration narrowness, average shear layer thickness, and number of serrations. Subsequently, these individual parameters were varied independently, as well as simultaneously, to understand their comparative stability implications. It was found that deeper serrations and higher chevron count reduce the growth rate of the K-H instability while mildly enhancing the phase speed. Although an explicit connection was not made, it was hypothesized that reduction in growth rate and phase speed of the instability should reduce the overall strength of the coherent structures as well as their radiation efficiency, thereby contributing to a reduction in mixing noise.

The above LST-based analysis does not account for the streamwise variation of the mean flow. Also, no link was established between the chevron geometry (something that can be designed) and the mean flow profile modifications (something that cannot be effected directly). In this paper, we attempt to fill these gaps. We use RANS to obtain the mean flow field for various chevron geometries. Subsequently, PSE is applied to them to determine the modifications in the instability wavepackets.

The far acoustic field can be obtained using a Kirchoff surface technique (or a Ffowcs-Williams Hawkings approach) if the near-field hydrodynamic pressure is known.[28] The foregoing instability wave analysis yields an average description of the coherent pressure field. While this is sufficient to obtain a good approximation of the far field for supersonic jets,[18] subsonic jets are more difficult to address. This has been observed in several studies,[29,30] and is attributed to the important effect of coherence decay (or wavepacket jitter) in the actual wavepackets. This is a particular issue in subsonic jets, since they are otherwise much quieter than supersonic jets.[11]

In this paper, we do not attempt to directly predict the far acoustic field. Instead, we hypothesize that the spectrum of perturbations within the exiting boundary layer is going to be similar irrespective of the particular chevron geometry. This is motivated by observations of a flat power spectral density of velocity fluctuations at the lip line near the nozzle of axisymmetric jets.[17] Then, the different chevron geometries will create different mean flow fields that will tend to result in differential streamwise evolution of the same perturbations. By studying these differences, we would be able to assess the relative strength and radiation efficiency of the near-field pressure in the respective jets. The near-field pressure, modulated by the jitter (assumed to affect all jets similarly), will transfer these differences to the far acoustic field. We recognize that the incoherence (jitter) may be more in cases of chevrons with greater impingement (due to enhanced mixing near the nozzle), but our current methodology does not account for this.

II. Linear parabolized stability equations for serrated jets

The parabolized stability equations (PSE) were proposed by Bertolotti and Herbert[23] as an efficient means of accounting for a slow variation of the base flow in the streamwise direction that is otherwise assumed to be unchanging in the classical spatial linear stability theory (LST). In LST, the ansatz for the stability solution is a (uniformly growing or decaying) wave in the stream direction, say x direction. On the other hand, the ansatz in PSE is a slowly-varying (in x) shape function that modulates the wave-like part; the latter is defined as in LST, but its complex wavenumber is also allowed a slow variation in x.

The PSE theory was originally applied to study transition for laminar base flows (the traditional use of LST). However, of late, linear PSE has been applied to model the naturally-occuring wavepackets (coherent structures in frequency domain) in free shear flows as linear instabilities of the *turbulent* mean flow.[16,11] This analysis hypothesizes a separation of scales between the low-frequency, low-spanwise (or azimuthal)

American Institute of Aeronautics and Astronautics

wavenumber wavepackets and the remaining incoherent fluctuations in turbulence. Moreover, it hypothesizes that the former are *linear* perturbations on the mean flow, which in turn is established by the fine-scale fluctuations through the energy cascade. Although these hypotheses haven't been proven formally, the PSE models have been distinctly successful in predicting the coherent fluctuations observed in high-speed high-Reynolds number jets.[16,17,18,21]

For details of the linear PSE theory, the reader is referred to Refs. [16,18,21]; here we give a very brief description. The flow field of the jet is described in cylindrical coordinates $\boldsymbol{x} = (x, r, \theta)$ by $\boldsymbol{q} = (u_x, u_r, u_\theta, p, \zeta)^{\mathrm{T}}$, which respectively denote the axial, radial and azimuthal components of velocity, pressure, and specific volume. Stability analysis decomposes $\boldsymbol{q}$ into a steady base flow $\overline{\boldsymbol{q}}$ (herein it is the turbulent mean flow), and the residual fluctuations $\boldsymbol{q}'$. Given the time-stationarity and azimuthal periodicity of the fluctuations, PSE represents them with the ansatz

$$\boldsymbol{q}'(\boldsymbol{x}, t) = \hat{\boldsymbol{q}}_\omega(\boldsymbol{x})\, \mathrm{e}^{-\mathrm{i}\omega t} + \text{c.c.}, \quad \hat{\boldsymbol{q}}_\omega(\boldsymbol{x}) = \underbrace{\mathrm{e}^{\mathrm{i} \int_{x_0}^{x} \alpha_\omega(\xi)\mathrm{d}\xi}}_{=:\chi_\omega(x)} \breve{\boldsymbol{q}}_\omega(x, r, \theta), \quad \breve{\boldsymbol{q}}_\omega(x, r, \theta) = \sum_{m=-\infty}^{\infty} \tilde{\boldsymbol{q}}_{\omega,m}(x, r)\, \mathrm{e}^{\mathrm{i}m\theta}. \quad (1)$$

In the above, $\hat{\boldsymbol{q}}$ is the temporal Fourier coefficient of $\boldsymbol{q}'$, with circular frequency ω. It is decomposed into the shape function $\breve{\boldsymbol{q}}$, and wave part χ (with variable wavenumber α). Finally, $\tilde{\boldsymbol{q}}$ is the azimuthal Fourier coefficient of $\breve{\boldsymbol{q}}$, with azimuthal mode number m.

The above ansatz, when substituted in the governing equations (compressible Navier Stokes equations in cylindrical coordinates) linearized about the base flow $\overline{\boldsymbol{q}}$, yields a set PDEs (in x and r) that are coupled by the azimuthal Fourier mode m. However, the assumption of slow variation in x renders them approximately parabolic in the covectively-unstable flows under consideration,[23] so that they can be marched in x starting from an initial condition at x_0 (generally near the nozzle) using step sizes that are restricted in their lower bound.[31] The initial condition is invariably the unstable Kelvin-Helmholtz mode found in the parallel-flow LST applied to the mean flow profile at x_0.

The chevrons, say L in number, are invariably arrayed uniformly around the circumference of the nozzle, so that the mean flow of the resulting jet has corresponding L-fold rotational symmetry. Moreover, the individual chevrons have a symmetry plane (they are like isosceles triangles), so that the mean flow also has mirror symmetry. Using this, it can be shown that the azimuthal Fourier modes of the linear instabilities have a sparse coupling.[20,21] That is, the instability solution can be separated into $\lceil (L+1)/2 \rceil$ independent 'azimuthal orders', indexed by M

$$\hat{\boldsymbol{q}}_\omega^M(x, r, \theta) = \chi_\omega(x) \sum_{l=-\infty}^{\infty} \tilde{\boldsymbol{q}}_{\omega, M-Ll}(x, r)\, \mathrm{e}^{\mathrm{i}(M-Ll)\theta}, \qquad M \in \{0, 1, \ldots, \lceil (L-1)/2 \rceil\}. \quad (2)$$

III.   RANS model of jets issuing from serrated nozzle

The linear PSE analysis of interest here requires the mean (time-averaged) turbulent flow field as its only input. RANS simulations are ideally suited for this purpose. Below we describe various aspects of the numerical computations.

A.   Specifying the geometry of the chevrons

Since we intend to determine the mean flow fields for a family of chevron nozzle geometries, particular attention is given to device a robust and re-usable procedure for creating the geometries. As discussed earlier, the primary parameters of the chevron are its impingement depth I, length L (or equivalently included angle), and chevron count N.

A MATLAB® code is written that accepts the values of these parameters and writes out the salient points on the chevron edges. The main round nozzle body is adpoted from the NASA geometry for the SMC series converging nozzles (see fig. 1(a)). In the tip plane of the chevron, it is assumed to form a parabola that smoothly continues from the round nozzle body upstream of it (half-cone angle of $5°$). The definitions of points 'A' and 'B' at the chevron root's inner and outer surfaces (see fig. 1(c)) are adopted from the NASA geometry, and are held constant throughout the subsequent chevron modifications. The point 'C' on the chevron tip varies depending on its impingement and length. The side faces of the chevron are cut by virtual planes thru the points 'A', 'B' and 'C'. The results of this exercise are compared to the NASA geometry for

American Institute of Aeronautics and Astronautics
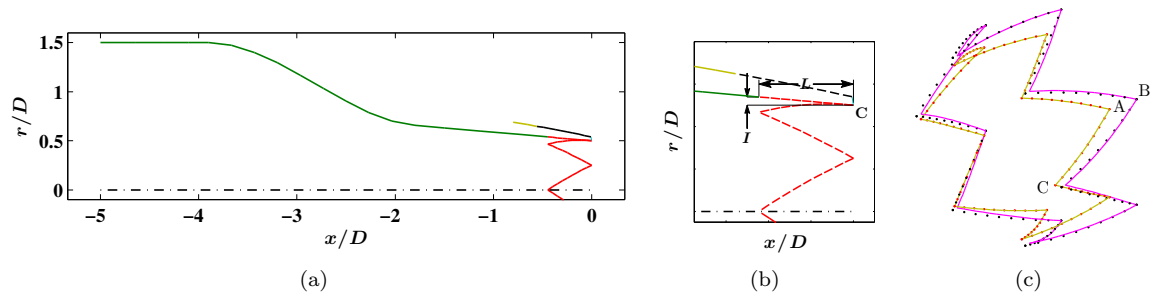
Figure 1. **(a)** Round nozzle body (green: inside surface; yellow: outside surface) with SMC001 chevron nozzle at its end shown in the tip plane. **(b)** Zoomed view showing length L and impingement I of chevron in the tip plane. **(c)** Comparison of original NASA SMC001 geometry (solid lines) with present model (markers).
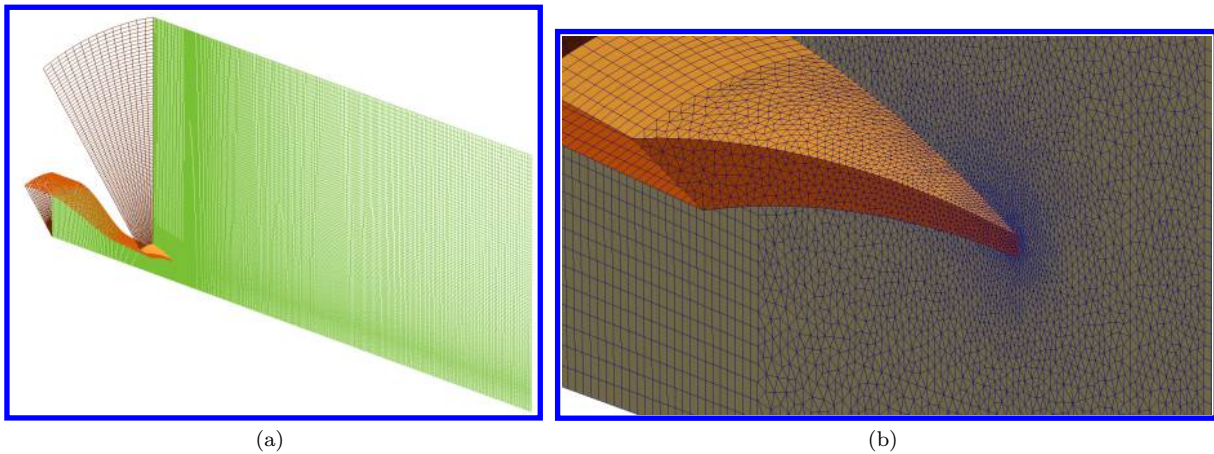
Figure 2. **(a)** Overall mesh and **(b)** zoomed view of chevron lip region for the minimal sector of the SMC001 case. The mesh coloring and opacity are different in the two figures to highlight the details. The mesh in the tip plane shown is representative of the local refinement.

the SMC001 chevron nozzle in fig. 1(c). The inner surface of the chevron is an excellent match. The outer surface is not replicated as well, but this is not a concern since it is in the essentially stagnant region. The chevron impingement, length and count can be varied parametrically independent of each other.

B.   The mesh

The mesh is created in Gmsh.[32] The geometry points on the nozzle body and chevron defined in the previous step are imported into Gmsh, and the connecting curves are defined programmatically. The overall mesh design follows the presentation in Ref. 33, with structured grid in the most part and unstructured grid around the chevron. A typical result is shown in fig. 2. The mesh resolution is specified at the lip where it is the minimum (in fig. 2 the minimum cell side is 0.001 times the nominal jet diameter); everywhere else the mesh scales linearly with this (including the azimuthal grid resolution).

The downstream extent of the domain from the nozzle exit is $15D$, whereas the radial extent is $6D$. We verified that the mean flow results are substantially independent of these choices. The minimal sector of the flow domain containing one half of a chevron is meshed, exploiting the rotational and mirror symmetry of the geometry (and hence the mean flow field).

C.   RANS simulations

Most RANS models were originally developed for wall-bounded flows, so that further modifications were necessary in applications to free shear flows, especially jets. Some of the well-known modifications to the $k - \epsilon$ model proposed for high-speed round jets, both cold and hot, can be found in Ref. 34, 35, 36. However,
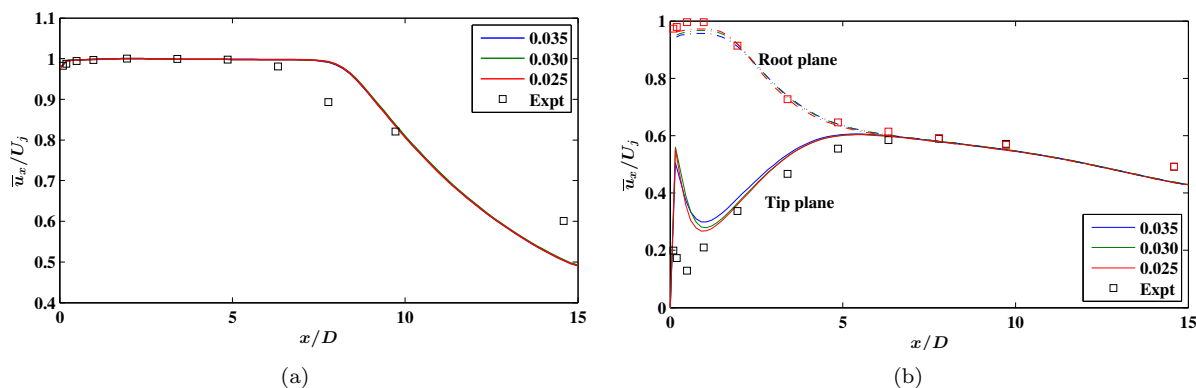
Figure 3. Comparison of RANS results with experiments of the SMC001 case in terms of mean axial velocity along (a) the centerline, and (b) the lip-line, the latter in both the tip and root planes of the chevron. RANS simulations were performed on successively finer grids, with the numbers in the legends indicating the minimum grid resolution (obtained at the lip of the nozzle) in terms of the nominal jet diameter.

the underlying hypothesis in these modifications, viz. the importance of Pope's[34] vortex stretching term, has been found to be questionable in more complex jets, like the serrated jets under consideration here.[37,38] Instead, a number of more sophisticated RANS models have been proposed, with particular applicability to serrated jets.[38,39,40] In our preliminary RANS simulations reported here, we have adopted the standard $k - \epsilon$ model;[41] it was also found to be the most appropriate for RANS simulations of serrated jets required for noise prediction using the acoustic analogy approach.[9]

All simulations reported here were performed using the open-source CFD package OpenFOAM.[42] The `rhoSimpleFoam` solver was used, which is a steady-state SIMPLE solver for RANS of compressible flows. The inlet is a velocity-inlet boundary, with pressure specified as zero-gradient and temperature specified as ambient (293 K). The outlet has OpenFOAM's `inletOutlet` condition which allows smooth outflow, with the pressure set to atmospheric (100 kPa). A `totalPressure` condition is specified on the radially-outward surface to allow entrainment. On the nozzle walls, we use the standard wall functions available for k and ϵ[41] in OpenFOAM. The side walls of the sector have a `symmetry` boundary condition.

IV.   RANS validation results

We first determine the closeness of the RANS simulation results with experimental data. In this regard, we use the database created at NASA SHJAR in extensive parametric testing of chevron nozzles.[1] In particular, the jet operating conditions are as follows (the 'SP7' setpoint): acoustic Mach no. 0.9, exit temperature ratio of 0.84, exit Reynolds number of 1.6×10^6. Of the several chevron geometries tested at NASA, we choose the SMC001 case for the validation exercise (this was also described in § III).

The SMC series of nozzles were made interchangeable. The (baseline) round nozzle (SMC000) had an exit diameter of 50.8 mm, and continued the 5° half-cone angle of the main nozzle body (see fig. 1(a)). The SMC001 nozzle differed from the round nozzle only insofar as 6 serrations were cut into it (they continued the 5° taper angle from the main nozzle body). Thus, the tips of the SMC001 chevron are on a circle of diameter 50.8 mm. In the following, length dimensions are normalized by the nominal nozzle exit diameter, D, of the baseline round nozzle. The impingement and length of each chevron are $0.04D$ and $0.445D$.

The simulations were performed on three progressively finer grids, with the minimum cell size as reported; the corresponding number of cells was 0.07, 0.11 and 0.19 million. Figure 3 presents the centerline and lip-line ($r = 0.5D$) axial velocity from the simulation and experiments. The grid convergence is satisfactory, except near the nozzle in the chevron tip plane. The length of the potential core as well as the decay region are not replicated very closely; however, such discrepancies have been noted in most previous studies.[38,39,40,33] The lip-line profiles, both along the root and tip planes of the chevron, are matched better.

The reader will recall that the purpose of our RANS simulations is to find *changes* in the mean flow field of the jet with modifications of the chevron geometry. As such, the above discrepancies are deemed acceptable in this preliminary study.

American Institute of Aeronautics and Astronautics
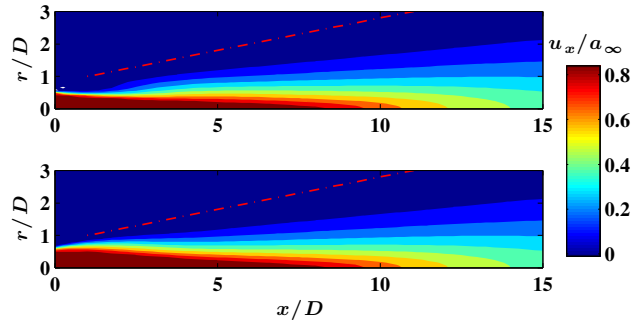
Figure 4. Mean streamwise velocity contours in chevron tip plane (top panel) and chevron root plane (bottom panel) for SMC001 case. The red line represents the virtual conical microphone array discussed in § VI.

Case	Impingement, I	Count, N	Length, L
Case 1 (SMC001)[1]	$0.04D$	6	$0.445D$
Case 2 (SMC006)[1]	$0.14D$	6	$0.445D$
Case 3	$0.04D$	10	$0.445D$

Table 1. Chevron geometry modifications evaluated.

For purposes of visualization, fig. 4 presents contours of the mean streamwise velocity for the foregoing case in two salient planes. The shear layer is pressed in radially in the plane of the chevron tips, whereas it bulges out in the plane of the chevron roots.

V.   PSE results for experimental vs. RANS mean flows

Another step in the validation process is the comparison of PSE results between the experimental and simulated mean flows in the SMC001 SP7 case. The PSE calculations are initiated at $x = 1D$. The results are shown in fig. 5, for a range of instability frequencies ($St = 0.20$, 0.35, and 0.50) and azimuthal orders ($M = 0$ and 1). We depict the least order azimuthal modes that are coupled in the solution ($m = 0$ and 1 respectively). The hydrodynamic pressure field displays the underlying coherent wavepacket nature of the turbulent jet most clearly,[15, 11] and its real part is presented. Although the RANS result displays a slightly, but consistently, larger wavelength, the overall comparison is quite satisfactory. This indicates that the discrepancies in the mean flow fields described in § IV may not detract from the general conclusions of the present approach.

We point to a few characteristics of the instability wavepackets in the serrated jets. As the frequency increases, the wavelength of the wavepackets decrease, as expected for an approximately constant convective velocity. Moreover, the wavepackets peak closer to the nozzle exit and decay earlier. The $m = 1$ mode displays a consistent delay in the decay behaviour compared to the corresponding $m = 0$ mode. These properties of the wavepackets are well known for round jets. Since the serrated jet becomes essentially round downstream, it is not surprising that it displays a similarity in the overall behaviour of wavepackets.

VI.   Effect of chevron geometry variations on instability wavepackets

We assess the effect of chevron geometry modifications through three variants, as listed in table 1. Cases 1 and 2 are respectively the SMC001 and SMC006 nozzles of Ref. 1, the latter having more aggressive impingement. 'Case 3' differs from 'Case 1' only in the chevron count. The chevron length was found to be irrelevant for the radiated noise in Ref. 1, and is therefore maintained constant in this preliminary assay. Through all these calculations, we maintain unity stagnation temperature ratio and exit acoustic Mach number of 0.9 (the 'SP7' set-point of Ref. 43 and Ref. 1).

Ref. 1 reported that the SMC006 nozzle is quieter than the SMC001 by 3-5 dB as far as aft angle low-
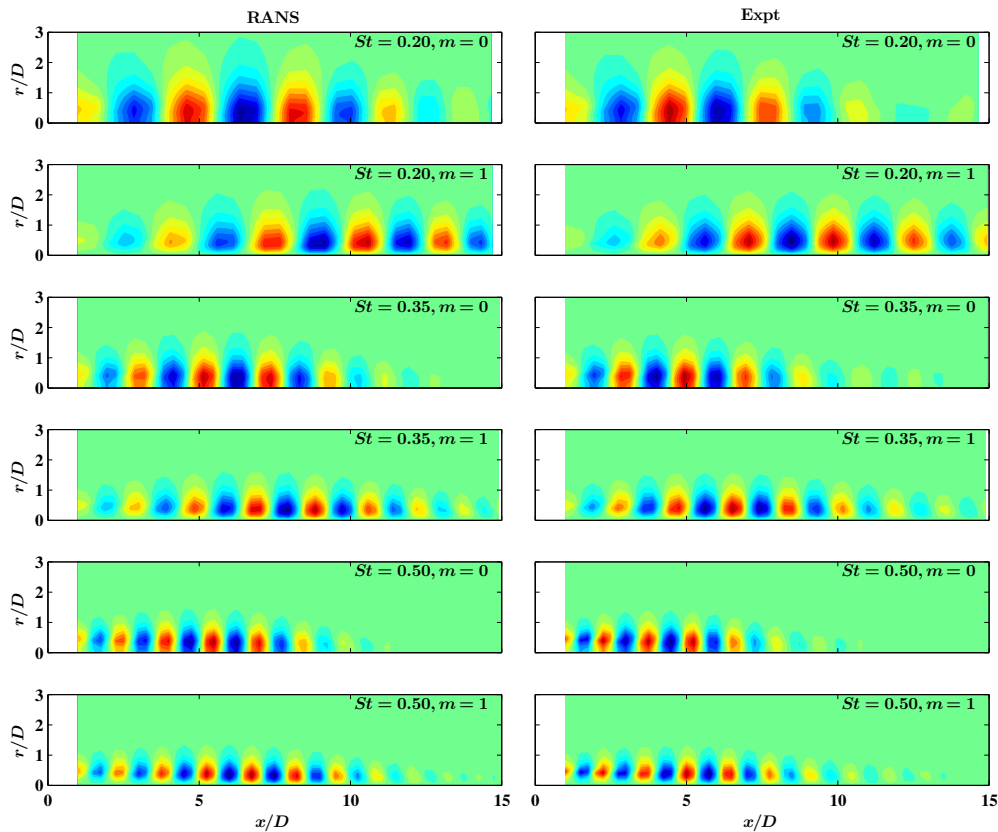
Figure 5. Comparison of PSE results for SMC001 case using mean flows from RANS and experiments (Expt). The real parts of the least order azimuthal modes of pressure that are coupled in the solution are shown. All fields are normalized to the same range (they take values from −1 to +1).

frequency noise is concerned. (It will be recalled that this is the loudest component of jet mixing noise.) There is a high-frequency penalty, especially at sideline angles. In Ref. 1, the effect of chevron count was studied while maintaining the notional 'vorticity strength' parameter constant. In this case, a higher chevron count (in particular, 10 chevrons) was associated with reduced effectiveness (the acoustic far field became indistinguishable from the round nozzle case). In the present work, we hold the chevron impingement and length constant when varying the chevron count.

The pressure component of the PSE solution for the instability wavepackets are shown for the three chevron geometry variants in fig. 6. The $St - m$ pairs depicted fall in the range of the loudest components of aft-angle mixing noise. Between the first two columns, the chevron impingement (I) has been increased keeping other parameters constant. Between the first and last columns, only the chevron count has been increased. Grossly, the overall pattern of the wavepackets are similar in the three cases. However, closer comparison of the first two columns reveals that the wavepackets tend to be less amplified (w.r.t. their near-nozzle amplitude) and saturate and decay earlier when the impingement is increased. The reverse trend is observed when the chevron count is increased (compare the first column with the third).

Ref. 15 established the relevance of studying the irrotational near-field pressure for understanding far-field acoustics. Indeed, the pressure information on a phased microphone array placed in this region can be used to calculate the far acoustic field in a Kirchhoff-surface procedure.[28] In a well-known experimental campaign conducted at NASA's Small Hot Jet Acoustic Rig, the near-field pressure was recorded on a 78-microphone phased array arranged in a conical fashion around the jet plume for a large range of jet operating conditions.[15] We extract the PSE pressure solution on a similar cone array (shown in fig. 4) – it has a half-cone angle of 11.3° and intersects the nozzle exit plane ($x - 0$) at $r = 0.8D$. As discussed in § I, the actual acoustic prediction from the PSE solution extracted on such a virtual microphone array is problematic, especially for the subsonic jets under investigation here. However, the overall amplitude of pressure fluctuations recorded on such an array is undoubtedly directly correlated with the far-field acoustic sound level.

American Institute of Aeronautics and Astronautics
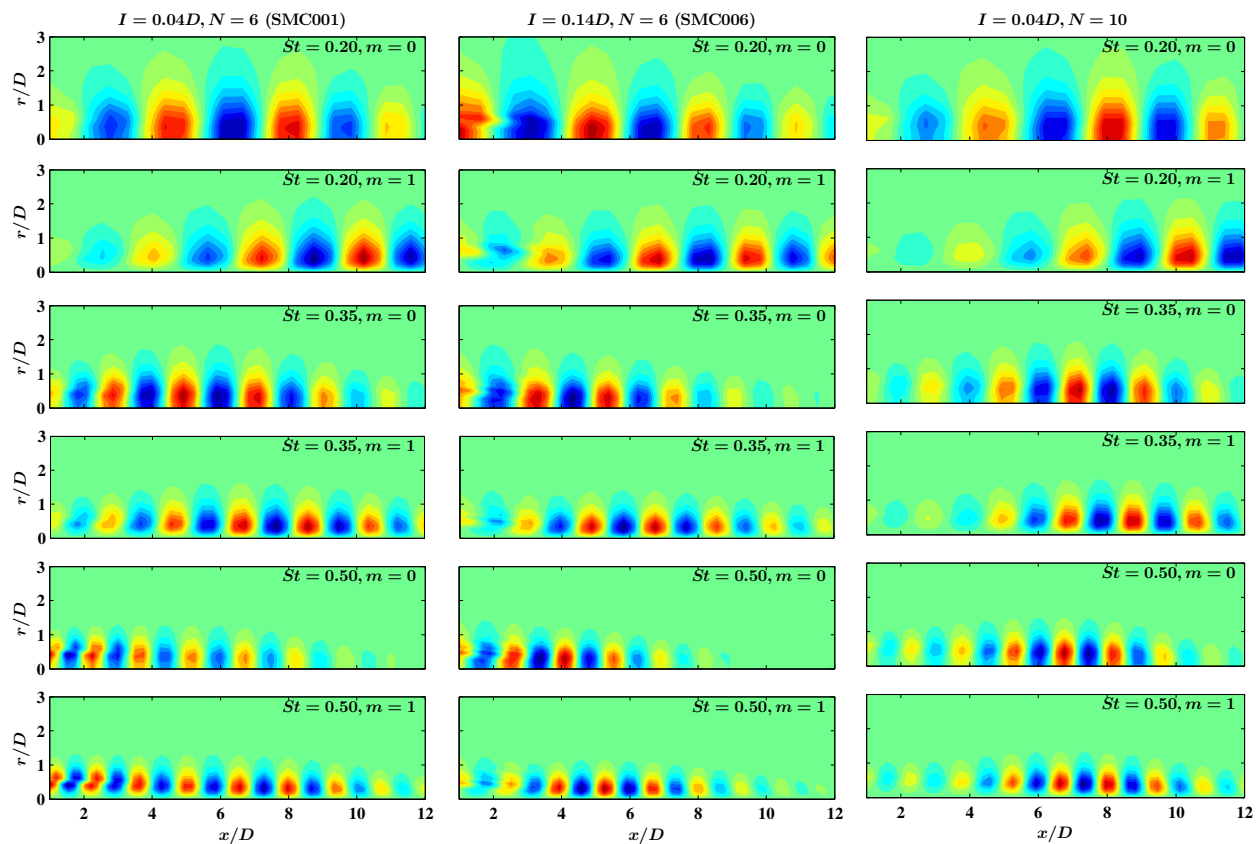
Figure 6. Effect of three chevron geometry modifications (one in each column) on the instability wavepackets in various $St - m$ pairs. The pressure PSE solution is shown following the scheme of fig. 5.

Therefore, while the results in fig. 6 have the expected trends (as discussed presently), fig. 7 presents a more pertinent quantitative comparison of the pressure amplitudes extracted on the above-mentioned cone array. Pursuant to our hypothesis that the fluctuations in the shear layer at the nozzle exit have a universal character (governed by the boundary layer at the nozzle lip), we scale all the wavepacket solutions to have unity pressure amplitude at the initial PSE station ($x = 1D$). In this setting, we note that deeper impingement of the chevrons results in a weaker wavepacket in all $St - m$ pairs. We can correlate this to a reduced radiation of these components (that are the loudest in the aft angles), which agrees well with the experimental findings of Ref. 1 described aobve. Conversely, increased chevron count generally leads to stronger wavepackets, again in agreement with acoustics experiments.

VII. Conclusions

In this paper, we attempt an understanding of the modifications of the linear instability waves in a serrated jet due to changes in the chevron geometries. The motivation is a reduced-order description of chevron jet noise in order to design the optimal chevron nozzle for mixing noise mitigation. We use RANS to obtain the mean flow fields due to various chevron geometries in a high subsonic cold jet. Subsequently, linear parabolized stability equations (PSE) is used to understand the consequent changes in the downstream evolution of the low-frequency and low-azimuthal Fourier mode instability waves that are responsible for the dominant aft angle noise radiation in jets.

We vary two independent parameters of the chevron – their impingement into the shear layer and their count. Increasing the impingement results in enhanced mixing that thickens the shear layer on an average while making it more lobed near the nozzle. This is found to weaken the instability wavepackets in the pertinent range of low-frequency and low-azimuthal Fourier modes. Increasing the chevron count results in stronger instability wavepackets in these Fourier modes. Both trends agree very well with the experimental

American Institute of Aeronautics and Astronautics
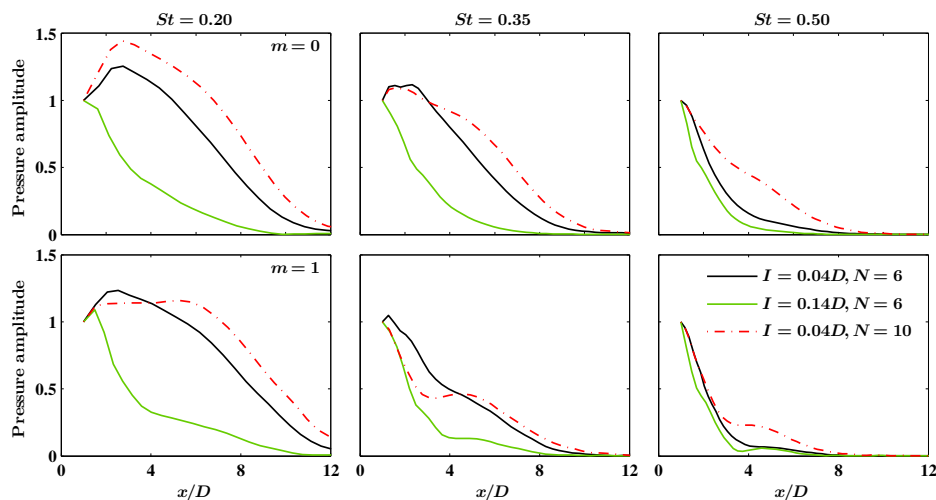
Figure 7. Effect of chevron modifications on the amplitudes of the instability wavepackets measured on a virtual conical microphone array in the irrotational near field. The top and bottom rows respectively present the $m = 0$ and $m = 1$ mode solutions, whereas each column displays a separate St mode. All wavepackets are scaled to have unity amplitude at the initial axial station ($x = 1D$).

findings of Ref. 1 regarding the corresponding acoustic effects of these chevron geometry modifications.

Given the encouraging qualitative performance of the proposed RANS-PSE approach, it can be used in the future to design chevron nozzles for optimized noise reduction. Following our findings in supersonic round jets,[18] quantitative predictions of noise reduction may be expected for supersonic jets issuing from chevron nozzles. For subsonic chevron jets, the estimates will be approximate. Finally, the thrust penalty of the chevron nozzles may be evaluated from the time-averaged flow field obtained in the intermediate RANS calculations, so that the optimization may also be informed by this crucial performance criterion.

References

[1]Bridges, J. E. and Brown, C. A., "Parametric testing of chevrons on single flow hot jets," *10th AIAA/CEAS Aeroacoustics Conference, AIAA Paper 2824*, 2004.

[2]Mengle, V. G., Elkoby, R., Brusniak, L., and Thomas, R. H., "Reducing propulsion airframe aeroacoustic interactions with uniquely tailored chevrons: 1. isolated nozzles," *12th AIAA/CEAS Aeroacoustics Conference, AIAA Paper 2467*, 2006.

[3]Alkislar, M. B., Krothapalli, A., and Butler, G. W., "The effect of streamwise vortices on the aeroacoustics of a Mach 0.9 jet," *Journal of Fluid Mechanics*, Vol. 578, 2007, pp. 139–169.

[4]Schlinker, R. H., Simonich, J. C., and Reba, R., "Flight effects on supersonic jet noise from chevron nozzles," *17th AIAA/CEAS Aeroacoustics Conference, AIAA Paper 2703*, 2011.

[5]Xia, H., Tucker, P. G., Eastwood, S., and Mahak, M., "The influence of geometry on jet plume development," *Prog. Aerosp. Sci.*, Vol. 52, 2012, pp. 56–66.

[6]Uzun, A. and Hussaini, M. Y., "Some issues in large-eddy simulations for chevron nozzle jet flows," *Journal of Propulsion and Power*, Vol. 28, No. 2, 2012, pp. 246–258.

[7]Brès, G. A., Nichols, J. W., Lele, S. K., Ham, F. E., Schlinker, R. H., Reba, R., and Simonich, J. C., "Unstructured large eddy simulation of a hot supersonic over-expanded jet with chevrons," *18th AIAA/CEAS Aeroacoustics Conference, AIAA Paper 2213*, 2012.

[8]Miller, S. A. E., "Toward a comprehensive model of jet noise using an acoustic analogy," *AIAA Journal*, Vol. 52, No. 10, 2014, pp. 2143–2164.

[9]Depuru Mohan, N. K., Dowling, A. P., Karabasov, S. A., Xia, H., Graham, O., Hynes, T. P., and Tucker, P. G., "Acoustic sources and far-field noise of chevron and round jets," *AIAA Journal*, Vol. 53, No. 9, 2015, pp. 2421–2436.

[10]Cavalieri, A. V. G., Jordan, P., Colonius, T., and Gervais, Y., "Axisymmetric superdirectivity in subsonic jets," *Journal of Fluid Mechanics*, Vol. 704, 2012, pp. 388–420.

[11]Jordan, P. and Colonius, T., "Wave packets and turbulent jet noise," *Annu. Rev. Fluid Mech.*, Vol. 45, 2013, pp. 173–195.

[12]Crighton, D. G. and Gaster, M., "Stability of slowly diverging jet flow," *Journal of Fluid Mechanics*, Vol. 77, No. 2, 1976, pp. 397–413.

American Institute of Aeronautics and Astronautics

[13]Mankbadi, R. and Liu, J. T. C., "Sound generated aerodynamically revisited: large-scale structures in a turbulent jet as a source of sound," *Proc. R. Soc. Lond. A*, Vol. 311, No. 1516, 1984, pp. 183–217.

[14]Tam, C. K. W. and Burton, D. E., "Sound generated by instability waves of supersonic flows. Part 2. Axisymmetric jets," *Journal of Fluid Mechanics*, Vol. 138, 1984, pp. 273–295.

[15]Suzuki, T. and Colonius, T., "Instability waves in a subsonic round jet detected using a near-field phased microphone array," *Journal of Fluid Mechanics*, Vol. 565, 2006, pp. 197–226.

[16]Gudmundsson, K. and Colonius, T., "Instability wave models for the near-field fluctuations of turbulent jets," *Journal of Fluid Mechanics*, Vol. 689, 2011, pp. 97–128.

[17]Cavalieri, A. V. G., Rodríguez, D., Jordan, P., Colonius, T., and Gervais, Y., "Wavepackets in the velocity field of turbulent jets," *Journal of Fluid Mechanics*, Vol. 730, 2013, pp. 559–592.

[18]Sinha, A., Rodríguez, D., Brès, G., and Colonius, T., "Wavepacket models for supersonic jet noise," *Journal of Fluid Mechanics*, Vol. 742, 2014, pp. 71–95.

[19]Léon, O. and Brazier, J.-P., "Investigation of the near and far pressure fields of dual–stream jets using an Euler–based PSE model," *19th AIAA/CEAS Aeroacoustics Conference, AIAA Paper 2839*, 2013.

[20]Gudmundsson, K. and Colonius, T., "Spatial stability analysis of chevron jet profiles," *13th AIAA/CEAS Aeroacoustics Conference, AIAA Paper 3599*, 2007.

[21]Sinha, A., Gudmundsson, K., Xia, H., and Colonius, T., "Parabolized stability analysis of jets from serrated nozzles," *Journal of Fluid Mechanics*, Vol. 789, 2016, pp. 36–63.

[22]Nichols, J. W. and Lele, S. K., "Global modes and transient response of a cold supersonic jet," *Journal of Fluid Mechanics*, Vol. 669, 2011, pp. 225–241.

[23]Bertolotti, F. P. and Herbert, T., "Analysis of the linear stability of compressible boundary layers using the PSE," *Theoretical and Computational Fluid Dynamics*, Vol. 3, No. 2, 1991, pp. 117–124.

[24]Saric, W. S. and Nayfeh, A. H., "Nonparallel stability of boundary-layer flows," *Physics of Fluids*, Vol. 18, No. 8, 1975, pp. 945–950.

[25]Uzun, A., Alvi, F. S., Colonius, T., and Hussaini, M. Y., "Spatial stability analysis of subsonic jets modified for low-frequency noise reduction," *AIAA Journal*, Vol. 53, No. 8, 2015, pp. 2335–2358.

[26]Sinha, A. and Colonius, T., "Linear stability implications of mean flow variations in turbulent jets issuing from serrated nozzles," *21st AIAA/CEAS Aeroacoustics Conference, AIAA Paper 3125*, 2015.

[27]Lajús Jr., F. C., Deschamps, C. J., and Cavalieri, A. V. G., "Spatial stability characteristics of non-circular jets," *21st AIAA/CEAS Aeroacoustics Conference, AIAA Paper 2537*, 2015.

[28]Reba, R., Narayanan, S., and Colonius, T., "Wave-packet models for large-scale mixing noise," *International Journal of Aeroacoustics*, Vol. 9, No. 4-5, 2010, pp. 533–558.

[29]Cavalieri, A. V. G. and Agarwal, A., "Coherence decay and its impact on sound radiation by wavepackets," *Journal of Fluid Mechanics*, Vol. 748, 2014, pp. 399–415.

[30]Baqui, Y. B., Agarwal, A., Cavalieri, A. V. G., and Sinayoko, S., "A coherence-matched linear source mechanism for subsonic jet noise," *Journal of Fluid Mechanics*, Vol. 776, 2015, pp. 235–267.

[31]Li, F. and Malik, M. R., "Spectral analysis of parabolized stability equations," *Computers & Fluids*, Vol. 26, No. 3, 1997, pp. 279–297.

[32]Geuzaine, C. and Remacle, J.-F., "Gmsh: a three-dimensional finite element mesh generator with built-in pre- and post-processing facilities," *Int. J. Numer. Meth. Enrng.*, Vol. 79, No. 11, 2009, pp. 1309–1331.

[33]Kurbatskii, K. A., "Comparison of RANS turbulence models in numerical prediction of chevron nozzle jet flows," *47th AIAA Aerospace Sciences Meeting, AIAA Paper 499*, 2009.

[34]Pope, S. B., "An explanation of the turbulent round-jet/plane-jet anomaly," *AIAA Journal*, Vol. 16, No. 3, 1978, pp. 279–281.

[35]Thies, A. T. and Tam, C. K. W., "Computation of turbulent axisymmetric and nonaxisymmetric jet flows using the k-epsilon model," *AIAA journal*, Vol. 34, No. 2, 1996, pp. 309–316.

[36]Tam, C. K. W. and Ganesan, A., "Modified $k - \epsilon$ turbulence model for calculating hot jet mean flows and noise," *AIAA journal*, Vol. 42, No. 1, 2004, pp. 26–34.

[37]Lebedev, A. B., Lyubimov, A. D., Maslov, V. P., Mineev, B. I., Secundov, A. N., and & Birch, S. F., "The prediction of three-dimensional jet flows for noise applications," *8th AIAA/CEAS Aeroacoustics Conference, AIAA Paper 2422*, 2002.

[38]Birch, S. F., Lyubimov, D. A., Secundov, A. N., and Yakubovsky, K. Y., "Numerical modeling requirements for coaxial and chevron nozzle flows," *9th AIAA/CEAS Aeroacoustics Conference, AIAA Paper 3287*, 2003.

[39]Massey, S. J., Thomas, R. H., Abdol-Hamid, K. S., and Elmiligui, A., "Computational and experimental flowfield analyses of separate flow chevron nozzles and pylon interaction," *9th AIAA/CEAS Aeroacoustics Conference, AIAA Paper 3212*, 2003.

[40]Engblom, W. A., Khavaran, A., and Bridges, J. E., "Numerical prediction of chevron nozzle noise reduction using WIND-MGBK methodology," *10th AIAA/CEAS Aeroacoustics Conference, AIAA Paper 2979*, 2004.

[41]Launder, B. E. and Spalding, D. B., *Mathematical models of turbulence*, Academic Press, 1972.

[42]Weller, H. G., Tabor, G., Jasak, H., and Fureby, C., "A tensorial approach to computational continuum mechanics using object-oriented techniques," *Computers in Physics*, Vol. 12, No. 6, 1998, pp. 620–631.

[43]Tanna, H. K., "An experimental study of jet noise. Part I: turbulent mixing noise," *Journal of Sound and Vibration*, Vol. 50, No. 3, 1977, pp. 405–428.

American Institute of Aeronautics and Astronautics